



## The effect of noncollinearity of $^{15}\text{N}$ - $^1\text{H}$ dipolar and $^{15}\text{N}$ CSA tensors and rotational anisotropy on $^{15}\text{N}$ relaxation, CSA/dipolar cross correlation, and TROSY

David Fushman & David Cowburn\*

*The Rockefeller University, 1230 York Avenue, New York, NY 10021, U.S.A.*

Received 7 August 1998; Accepted 8 October 1998

*Key words:* anisotropic overall motion, chemical shift anisotropy, NMR relaxation, TROSY

### Abstract

Current approaches to  $^{15}\text{N}$  relaxation in proteins assume that the  $^{15}\text{N}$ - $^1\text{H}$  dipolar and  $^{15}\text{N}$  CSA tensors are collinear. We show theoretically that, when there is significant anisotropy of molecular rotation, different orientations of the two tensors, experimentally observed in proteins, nucleic acids, and small peptides, will result in differences in site-specific correlation functions and spectral densities. The standard treatments of the rates of longitudinal and transverse relaxation of amide  $^{15}\text{N}$  nuclei, of the  $^{15}\text{N}$  CSA/ $^{15}\text{N}$ - $^1\text{H}$  dipolar cross correlation, and of the TROSY experiment are extended to account for the effect of noncollinearity of the  $^{15}\text{N}$ - $^1\text{H}$  dipolar and  $^{15}\text{N}$  CSA (chemical shift anisotropy) tensors. This effect, proportional to the degree of anisotropy of the overall motion,  $(D_{\parallel}/D_{\perp} - 1)$ , is sensitive to the relative orientation of the two tensors and to the orientation of the peptide plane with respect to the diffusion coordinate frame. The effect is negligible at small degrees of anisotropy, but is predicted to become significant for  $D_{\parallel}/D_{\perp} \geq 1.5$ , and at high magnetic fields. The effect of noncollinearity of  $^{15}\text{N}$  CSA and  $^{15}\text{N}$ - $^1\text{H}$  dipolar interaction is sensitive to both gross (hydrodynamic) properties and atomic-level details of protein structure. Incorporation of this effect into relaxation data analysis is likely to improve both precision and accuracy of the derived characteristics of protein dynamics, especially at high magnetic fields and for molecules with a high degree of anisotropy of the overall motion. The effect will also make TROSY efficiency dependent on local orientation in moderately anisotropic systems.

### Introduction

NMR relaxation methods provide information about dynamics of macromolecules in solution, highly important for understanding various aspects of their structure and function. There is increasing interest in NMR relaxation studies stimulated by (a) emerging applications in structure determination of orientational dependence of relaxation rates, due to the anisotropy of the overall tumbling (Tjandra et al., 1997; Clore et al., 1998; Clore and Gronenborn, 1998); (b) advances in NMR applications to larger proteins based on relaxation-optimized approaches (Pervushin et al., 1997); (c) NMR relaxation methods of assessment of chemical shift tensors in solution (Fushman and

Cowburn, 1998; Fushman et al., 1998b); and (d) possible applications to estimation of segmental entropy (Akke et al., 1993; Yang and Kay, 1996). These applications require not only precise but also accurate analysis of NMR relaxation data. The currently established approaches and models (Kay et al., 1989; Peng and Wagner, 1992), which were designed and tested on  $^{15}\text{N}$  relaxation in small, mostly spherical proteins at moderate magnetic field strengths, require significant extensions in order to account for deviations from 'ideal' behavior, including anisotropy of overall rotation, site-specific variations in  $^{15}\text{N}$  CSA, etc.

Molecular motion causes nuclear spin relaxation in macromolecules via modulations of both the chemical shift tensor of the nucleus and the dipolar interactions

\*To whom correspondence should be addressed.

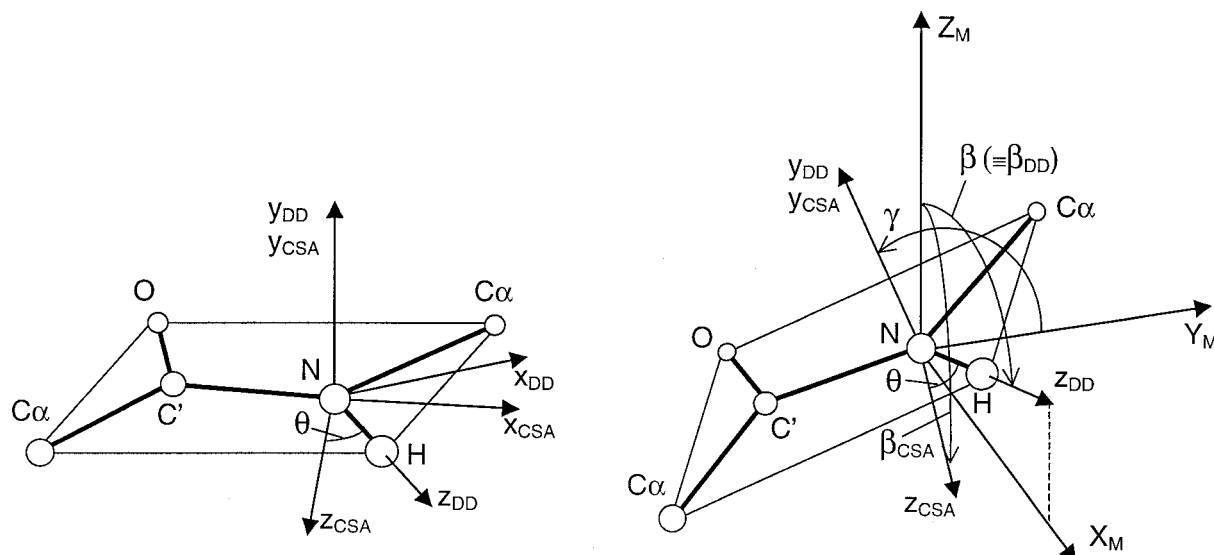


Figure 1. Definition of the Euler angles characterizing relative orientation of the  $^{15}\text{N}$ - $^1\text{H}$  dipolar and  $^{15}\text{N}$  CSA tensors with respect to the molecular frame,  $\mathbf{M}$ , defined by the principal axes of the overall rotational diffusion tensor of the molecule. The principal axes,  $x_{\text{CSA}}$ ,  $y_{\text{CSA}}$ , and  $z_{\text{CSA}}$ , of the CSA tensor,  $\text{CSA}$ , are defined here to be aligned with the most shielded ( $\sigma_{11}$ ), intermediate ( $\sigma_{22}$ ), and the least shielded ( $\sigma_{33}$ ) components, respectively, of the  $^{15}\text{N}$  chemical shift tensor. The  $y$ -axes of the dipolar and CSA tensors are assumed to be collinear, based on NMR data for peptides (see text). The  $\mathbf{M} \rightarrow \text{NH}$  transformation consists of rotation by angle  $\beta$  around the  $Y_{\text{M}}$  axis and a subsequent rotation around the new direction of the NH bond by an angle  $\gamma$ . The  $\text{NH} \rightarrow \text{CSA}$  transformation is a rotation around the  $Y_{\text{DD}} (= Y_{\text{CSA}})$  axis by an angle  $\theta$ . Positive values of the angles correspond to a counterclockwise rotation; therefore the relative orientation of  $Z_{\text{CSA}}$  and  $Z_{\text{NH}}$  observed in small peptides and proteins (as shown in the Figure) corresponds to negative values of  $\theta$  ( $\theta = -15.7^\circ \pm 5^\circ$  (Fushman et al., 1998b)).

of the nucleus with other, usually directly bonded, nuclei. In many cases, this modulation is simply re-orientation of the dipolar (DD) and chemical shift anisotropy (CSA) tensors with respect to the external magnetic field. These tensors are, in general, not collinear. Their relative orientation will influence the relaxation properties of the NMR observed nucleus, and therefore are of significance for obtaining an accurate picture of macromolecular dynamics from NMR relaxation data.

The existing approaches to  $^{15}\text{N}$ -relaxation data analysis usually assume that the principal axes of the  $^{15}\text{N}$ - $^1\text{H}$  dipolar and  $^{15}\text{N}$  CSA tensors have the same orientation. As has been shown by numerous solid state NMR studies on peptides (Harbison et al., 1984; Oas et al., 1987; Hartzell et al., 1987; Hiyama et al., 1988; Shoji et al., 1989; Mai et al., 1993) and recent NMR solution studies of proteins (Ottiger et al., 1997; Fushman et al., 1998b), the two tensors are not collinear. The noncollinearity is rather small (10–20°) and can probably be ignored in the case of small degrees of hydrodynamic anisotropy. This assumption might render the microdynamic parameters inaccurate, when applied to macromolecules with a significant degree of anisotropy, especially, at high magnetic fields,

where the size of contributions to relaxation from the two interactions become comparable.

In this paper, we assess the effect of noncollinearity of the  $^{15}\text{N}$ - $^1\text{H}$  dipolar and  $^{15}\text{N}$  CSA tensors on the  $^{15}\text{N}$  relaxation in proteins in solution.

## Theory

The  $^{15}\text{N}$  longitudinal ( $R_1$ ) and transverse ( $R_2$ ) relaxation rates in an isolated  $^{15}\text{N}$ - $^1\text{H}$  pair can be written in the following form (Abragam, 1961):

$$R_1 = 3d^2 J_{\text{DD}}(\omega_{\text{N}}) + c^2 J_{\text{CSA}}(\omega_{\text{N}}) + d^2 [J_{\text{DD}}(\omega_{\text{H}} - \omega_{\text{N}}) + 6J_{\text{DD}}(\omega_{\text{H}})] \quad (1)$$

$$R_2 = \frac{1}{2} \{ d^2 [4J_{\text{DD}}(0) + 3J_{\text{DD}}(\omega_{\text{N}})] + c^2 [4J_{\text{CSA}}(0) + 3J_{\text{CSA}}(\omega_{\text{N}})] + d^2 [J_{\text{DD}}(\omega_{\text{H}} - \omega_{\text{N}}) + 6J_{\text{DD}}(\omega_{\text{H}}) + 6J_{\text{DD}}(\omega_{\text{H}} + \omega_{\text{N}})] \} \quad (2)$$

where  $d = -(\mu_0 / (4\pi)) \gamma_{\text{H}} \gamma_{\text{N}} h / (4\pi r_{\text{HN}}^3)$ ,  $c = \gamma_{\text{N}} B_0 (\sigma_{\parallel} - \sigma_{\perp}) / 3$ ,  $r_{\text{HN}}$  is the internuclear  $^{15}\text{N}$ - $^1\text{H}$  dis-

tance,  $B_o$  is the magnetic field strength,  $\sigma_{\parallel} - \sigma_{\perp}$  is the anisotropy of the  $^{15}\text{N}$  chemical shift tensor,  $\gamma_H$ ,  $\gamma_N$  and  $\omega_H$ ,  $\omega_N$  are gyromagnetic ratios and resonance frequencies of the nuclei, and  $h$  is Planck's constant. The spectral density functions,  $J_{DD}(\omega)$  and  $J_{CSA}(\omega)$ , are Fourier transforms of the corresponding autocorrelation functions,  $C_{DD}(t)$  and  $C_{CSA}(t)$ , characterizing reorientation of the unique axis of the  $^{15}\text{N}$ - $^1\text{H}$  dipolar coupling (NH-vector), and of the unique axis of the  $^{15}\text{N}$  CSA tensor (CSA-vector), respectively. Axial symmetry of the  $^{15}\text{N}$  CSA tensor is assumed here; therefore, a unit vector along the unique axis (associated with the least shielded component) of the CSA tensor will be referred to as the CSA-vector. Note that terms describing cross correlation between the  $^{15}\text{N}$ - $^1\text{H}$  dipolar interaction and  $^{15}\text{N}$  CSA (see below) are omitted in Equations 1–2; these effects are usually suppressed in the experiment by using proper decoupling techniques (Kay et al., 1992; Palmer et al., 1992).

For the purpose of this paper we will neglect the effect of local dynamics of the macromolecule, considering only overall rigid body rotations of the molecule and assuming each of the vectors (NH, CSA) being fixed in its equilibrium orientation. Including local mobility introduces additional complexity in the picture, because of anisotropic character of the local dynamics in a protein (Fushman et al., 1994; Bremi et al., 1997; Fischer et al., 1997), which might result in local motion of the NH and CSA vectors characterized by different amplitudes (order parameters), as observed e.g. in molecular dynamics simulations (Chatfield et al., 1998; S. Pfeiffer, private communication). Assuming a relatively small angle between the two vectors and small amplitudes of local motion in the regions of well-defined secondary structure, these differences are likely to have small second order effects as compared to the one considered here.

Assuming an axial symmetry of the overall rotational diffusion tensor, the relevant autocorrelation functions can be written as (see e.g. Woessner, 1962)

$$C_V(t) = \frac{1}{5} \left\{ \frac{1}{4} e^{-t/\tau_1} (3 \cos^2 \beta_V - 1)^2 + 3 e^{-t/\tau_2} \cos^2 \beta_V \sin^2 \beta_V + \frac{3}{4} e^{-t/\tau_3} \sin^4 \beta_V \right\} \quad (3)$$

where  $V = \text{DD}$  or  $\text{CSA}$ ;  $\beta_{DD}$  and  $\beta_{CSA}$  are polar angles characterizing orientation of the NH and CSA vectors, respectively, with respect to the z-axis of the molecular frame  $\mathbf{M}$  defined by the principal axes of

the overall rotational diffusion tensor of the molecule (Figure 1); and

$$\begin{aligned} \tau_1^{-1} &= 6D_{\perp}; & \tau_2^{-1} &= 5D_{\perp} + D_{\parallel}; \\ \tau_3^{-1} &= 2D_{\perp} + 4D_{\parallel}; \end{aligned} \quad (4)$$

where  $D_{\parallel}$  and  $D_{\perp}$  denote principal values of the diffusion tensor. A similar treatment could be derived for the general case of a fully anisotropic tensor.

The noncollinearity of the  $^1\text{H}$ - $^{15}\text{N}$  dipolar and  $^{15}\text{N}$  CSA tensors will, in general, result in differences between the angles  $\beta_{DD}$  and  $\beta_{CSA}$  (Figure 1), hence  $C_{DD}(t) \neq C_{CSA}(t)$  and  $J_{DD}(\omega) \neq J_{CSA}(\omega)$ . To assess the difference between the two correlation functions, consider the transformation  $\mathbf{M} \rightarrow \mathbf{CSA}$  from the molecular frame to the local frame of the CSA tensor as a result of two subsequent transformations:  $\mathbf{M} \rightarrow \mathbf{NH}$  and  $\mathbf{NH} \rightarrow \mathbf{CSA}$  (Figure 1). Let  $\Omega_{M \rightarrow NH} \equiv \{\alpha, \beta, \gamma\}$  and  $\Omega_{NH \rightarrow CSA} \equiv \{\phi, \theta, \Psi\}$ , be sets of Euler angles describing orientation of the dipolar tensor with respect to the molecular frame  $\mathbf{M}$ , and of the CSA tensor with respect to the dipolar tensor coordinate frame, respectively. Note that  $\beta \equiv \beta_{DD}$ . Without loss of generality, angle  $\alpha$  can be set to zero for the axially symmetric diffusion tensor for overall rotation. Assuming axial symmetry of the  $^{15}\text{N}$  CSA tensor,  $\Psi$  can also be set to 0. Further simplification is possible based on the observation (Harbison et al., 1984; Hartzell et al., 1987; Oas et al., 1987; Hiyama et al., 1988; Mai et al., 1993) that the unique axis of the CSA tensor lies approximately in the peptide plane, with the y-axes of both dipolar and CSA tensors being almost collinear (Figure 1), i.e.  $\phi$  is zero. The orthogonality of one of the principal axes (here  $y_{CSA}$ ) of the chemical shielding tensor to the peptide plane is expected (Harbison et al., 1984; Oas et al., 1987) due to planar symmetry of the peptide bond. Of the three remaining variable, nonzero angles,  $\beta$  and  $\gamma$  characterize the orientation of the NH vector and of the peptide plane, respectively, with respect to the diffusion tensor frame, and  $\theta$  is the angle between the NH and CSA vectors (Figure 1). After the rotational transformations using the Wigner rotation matrices (Brink and Satchler, 1993), it can be shown that:

$$C_{CSA}(t) = C_{DD}(t) + \Delta C(t, D_{\parallel}, D_{\perp}, \beta, \gamma, \theta) \quad (5)$$

where  $C_{DD}(t)$  is given in Equation 3,

$$\Delta C(t, D_{\parallel}, D_{\perp}, \beta, \gamma, \theta) = \frac{3}{20} \left\{ (e^{-t/\tau_1} - e^{-t/\tau_2}) F_a(\beta, \gamma, \theta) - (e^{-t/\tau_2} - e^{-t/\tau_3}) F_b(\beta, \gamma, \theta) \right\} \quad (6)$$

and

$$F_a(\beta, \gamma, \theta) = \sin^2 \theta \cos^2 \beta (3 \sin^2 \beta - 3 \cos^2 \beta \sin^2 \theta - 1) - 4 \cos \gamma \sin \theta \cos \theta \sin \beta \cos \beta (3 \cos^2 \theta \cos^2 \beta - 1) + 2 \cos^2 \gamma \sin^2 \theta \sin^2 \beta (9 \cos^2 \theta \cos^2 \beta - 1) - 3 \cos^3 \gamma \sin^3 \theta \sin^3 \beta (4 \cos \theta \cos \beta - \cos \gamma \sin \theta \sin \beta) \quad (7)$$

$$F_b(\beta, \gamma, \theta) = \sin^2 \theta \cos^2 \beta (\sin^2 \beta - \cos^2 \beta \sin^2 \theta + 1) - 4 \cos \gamma \sin \theta \cos \theta \sin \beta \cos \beta (\cos^2 \theta \cos^2 \beta - 1) + 2 \cos^2 \gamma \sin^2 \theta \sin^2 \beta (3 \cos^2 \theta \cos^2 \beta - 1) - \cos^3 \gamma \sin^3 \theta \sin^3 \beta (4 \cos \theta \cos \beta - \cos \gamma \sin \theta \sin \beta)$$

Note that  $\Delta C$  can be positive or negative, while  $C_{CSA} = C_{DD} + \Delta C$  is always positive. As one can see from Equations 5–7, the difference between  $C_{CSA}(t)$  and  $C_{DD}(t)$ ,  $\Delta C$ , vanishes in the case of isotropic overall rotational diffusion ( $D_{\parallel} = D_{\perp}$ ;  $\tau_1 = \tau_2 = \tau_3$ ), as well as when the CSA and NH vectors become collinear ( $\theta = 0$ ). The relation  $C_{CSA}(t) \equiv C_{DD}(t)$  holds also for certain sets of  $\{\beta, \gamma\}$  values, e.g.  $\{90^\circ, 90^\circ\}$  (see Figure 2), which cause both NH and CSA vectors to have the same tilt angle towards the z-axis ( $D_{\parallel}$ ) of the diffusion tensor frame. Equations 1–2 can now be recast as follows:

$$R_1 = 3(d^2 + c^2)J_{DD}(\omega_N) + d^2[J_{DD}(\omega_H - \omega_N) + 6J_{DD}(\omega_H)] + 3c^2\Delta J(\omega_N, D_{\parallel}, D_{\perp}, \beta, \gamma, \theta) \quad (8)$$

$$R_2 = \frac{1}{2}\{(d^2 + c^2)[4J_{DD}(0) + 3J_{DD}(\omega_N)] + d^2[J_{DD}(\omega_H - \omega_N) + 6J_{DD}(\omega_H) + 6J_{DD}(\omega_H + \omega_N)]\} + \frac{1}{2}c^2[4\Delta J(0, D_{\parallel}, D_{\perp}, \beta, \gamma, \theta) + 3\Delta J(\omega_N, D_{\parallel}, D_{\perp}, \beta, \gamma, \theta)] \quad (9)$$

These expressions differ from the conventionally used equations for  $^{15}\text{N}$  relaxation rates only by the terms

$$\Delta J(\omega_N, D_{\parallel}, D_{\perp}, \beta, \gamma, \theta) = \frac{1}{20} \left( \frac{D_{\parallel}}{D_{\perp}} - 1 \right) \left[ \frac{1 - \omega^2 \tau_1 \tau_2}{1 + \omega^2 \tau_1^2} F_a(\beta, \gamma, \theta) - 3 \frac{\tau_3}{\tau_1} \frac{1 - \omega^2 \tau_2 \tau_3}{1 + \omega^2 \tau_3^2} F_b(\beta, \gamma, \theta) \right] \frac{\tau_2}{1 + \omega^2 \tau_2^2} \quad (10)$$

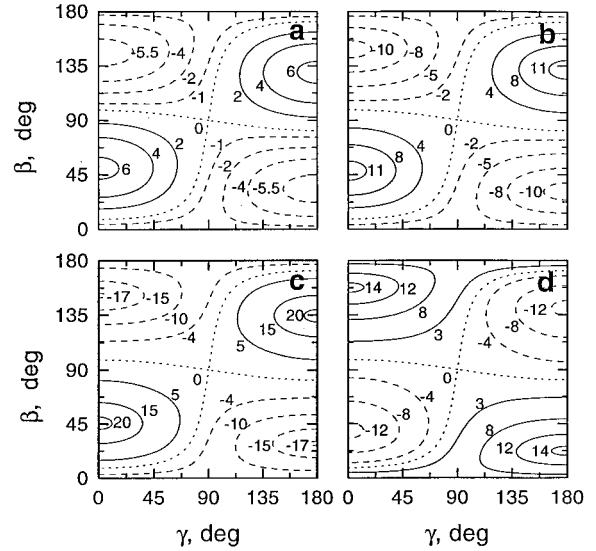


Figure 2. Contour map of relative percentile differences between  $J_{CSA}(\omega)$  and  $J_{DD}(\omega)$  for  $\omega = 0$  (a)–(c) and  $\omega = \omega_N$  (d), for various degrees of anisotropy: (a)  $D_{\parallel}/D_{\perp} = 1.5$ ; (b)  $D_{\parallel}/D_{\perp} = 2$ ; (c,d)  $D_{\parallel}/D_{\perp} = 3$ . Numbers indicate values of  $\Delta J(\omega)/J_{DD}(\omega)$  in percent. The calculations were performed for resonance frequency of 600 MHz assuming  $\theta = -17^\circ$  (Fushman et al., 1998b) and an overall correlation time of 5 ns. Solid and dashed lines indicate positive and negative values of  $\Delta J$ , respectively. Dotted lines correspond to loci of those  $\{\beta, \gamma\}$ -values for which both the NH and CSA vectors happen to have the same tilt angle from the z-axis (i.e.  $\theta$  corresponds to a pure rotation around the z-axis, hence  $C_{CSA}(t) = C_{DD}(t)$ ).

which are Fourier transforms of  $\Delta C(t, D_{\parallel}, D_{\perp}, \beta, \gamma, \theta)$ , Equations 5–7. As one can see from Equations 7 and 10, these additional terms scale as the degree of anisotropy of the overall motion,  $(D_{\parallel}/D_{\perp} - 1)$ , and vary, both in the magnitude and in sign, for various sets of  $\beta, \gamma$ , and  $\theta$ . As expected, the effect of noncollinearity of  $^{15}\text{N}$  CSA and  $^{15}\text{N}$ - $^1\text{H}$  dipolar interaction is sensitive to both the overall hydrodynamic properties,  $D_{\parallel}, D_{\perp}$ , and the atomic-level details of protein structure,  $\beta, \gamma$ , and the orientation of the CSA tensor,  $\theta$ .

Similar analysis applied to the cross correlation function (e.g. Fischer et al., 1997) between  $^{15}\text{N}$  CSA and  $^1\text{H}$ - $^{15}\text{N}$  dipolar interaction gives

$$C_{CROSS}(t) = C_{DD}(t)P_2(\cos \theta) + \Delta C_{CROSS}(t, D_{\parallel}, D_{\perp}, \beta, \gamma, \theta) \quad (11)$$

where  $P_2(x) = \frac{1}{2}(3x^2 - 1)$  is the second-rank Legendre polynomial, and  $\Delta C_{CROSS}$  is given by Equation 6, with

$$\begin{aligned}
F_a(\beta, \gamma, \theta) &= -\frac{1}{2} \sin \theta \sin \beta (4 \cos \theta \cos \beta \cos \gamma \\
&\quad - \sin \theta \sin \beta \cos 2\gamma)(3 \cos^2 \beta - 1) \\
F_b(\beta, \gamma, \theta) &= -\frac{1}{2} \sin \theta \sin^2 \beta [2 \cos \theta \sin 2\beta \cos \gamma \\
&\quad + \sin \theta \cos 2\gamma (\cos^2 \beta + 1)] \quad (12)
\end{aligned}$$

The cross correlation contribution to  $^{15}\text{N}$  relaxation (Goldman, 1984) can then be written in the following form:

$$\begin{aligned}
\eta &= dc[4J_{DD}(0) + 3J_{DD}(\omega_N)]P_2(\cos \theta) \\
&\quad + dc[4\Delta J_{\text{CROSS}}(0, D_{\parallel}, D_{\perp}, \beta, \gamma, \theta) \\
&\quad + 3\Delta J_{\text{CROSS}}(\omega_N, D_{\parallel}, D_{\perp}, \beta, \gamma, \theta)] \quad (13)
\end{aligned}$$

where the  $\Delta J_{\text{CROSS}}$  terms are Fourier transforms of  $\Delta C_{\text{CROSS}}(t, D_{\parallel}, D_{\perp}, \beta, \gamma, \theta)$  and can be represented by Equation 10 with  $F_a$  and  $F_b$  from Equation 12. In the case of weak rotational anisotropy and/or small angles  $\theta$ , the  $\Delta J_{\text{CROSS}}$  terms vanish, and Equation 13 reduces to the expression for  $\eta$  obtained by Tjandra et al. (1996).

## Results and discussion

The relevant spectral densities  $J_{DD}(\omega)$  and  $J_{\text{CSA}}(\omega)$  were calculated as a function of  $\beta$ ,  $\gamma$ , and  $\theta$  for various degrees of rotational anisotropy (Figures 2 and 3). As one can see, the effect is rather small for moderate degrees of anisotropy ( $D_{\parallel}/D_{\perp} < 1.5$ ). It increases with the angle  $\theta$ , as well as with  $D_{\parallel}/D_{\perp}$ , and, for  $J(\omega_N)$ , also with the resonance frequency, and with the overall correlation time (Figure 3). The regions of maximal effect correspond to  $\gamma$  values of 0 or  $180^\circ$ , i.e. when the peptide plane is parallel to the diffusion axis.

At magnetic field strengths currently available, the CSA contribution to  $^{15}\text{N}$  relaxation rates is smaller than the dipolar contribution (e.g.  $c^2/d^2 = 0.32$  at 600 MHz), therefore the relative contributions from the  $\Delta J$  terms to Equations 8 and 9 are small at moderate degrees of rotational anisotropy. Since  $c$  scales as  $B_0$ , the effect of noncollinearity on  $^{15}\text{N}$  relaxation rates increases with magnetic field (Figure 4) and is expected to become considerable at higher frequencies ( $\sim 1$  GHz), when the CSA contribution to  $^{15}\text{N}$  relaxation becomes comparable with the dipolar contribution. Even at 600 MHz, the effect is expected to be above the level of experimental errors in  $R_1$  and  $R_2$  determination ( $\sim 1\%$ ) for proteins with  $D_{\parallel}/D_{\perp} \geq 1.5$ , and  $\tau_c > 5$  ns.

For small values of the angle  $\theta$ , the effect depends approximately linearly on  $\theta$  (Figure 3). Variations of  $\pm 5^\circ$  in  $\theta$  values observed in proteins (Fushman et al., 1998b) will lead to  $\pm 25\%$  variations in the expected perturbing effect in the relaxation rates.

In those cases when the contribution from the non-collinearity is significant, a neglect of this effect in the relaxation data analysis might render the results of such analysis inaccurate.  $\Delta J(0, D_{\parallel}, D_{\perp}, \beta, \gamma, \theta)$  and  $\Delta J(\omega_N, D_{\parallel}, D_{\perp}, \beta, \gamma, \theta)$  are of opposite sign ( $\omega_N^2 \tau_1 \tau_2, \omega_N^2 \tau_2 \tau_3 > 1$ ), and so are the variations in  $R_2$  and  $R_1$  (Equations 8–10, Figure 2). The ratio of the two relaxation rates can be approximated from Equations 8 and 9, neglecting contributions from the high-frequency components,  $J(\omega_H)$ ,  $J(\omega_H \pm \omega_N)$ , of the spectral density function, as follows:

$$\begin{aligned}
\frac{2R_2 - R_1}{R_1} &= \frac{4J_{DD}(0)}{3J_{DD}(\omega_N)} \left[ 1 + \frac{c^2}{d^2 + c^2} \right. \\
&\quad \left( \frac{\Delta J(0, D_{\parallel}, D_{\perp}, \beta, \gamma, \theta)}{J_{DD}(0)} \right. \\
&\quad \left. \left. - \frac{\Delta J(\omega_N, D_{\parallel}, D_{\perp}, \beta, \gamma, \theta)}{J_{DD}(\omega_N)} \right) \right] \quad (14)
\end{aligned}$$

Therefore the primary effect of the neglect of non-collinearity is likely to be on the  $R_2/R_1$  ratio. This will affect accuracy and precision of the derived overall rotational properties including the principal values and/or orientation of the principal axes of the diffusion tensor. Since both  $R_1$  and  $R_2$  are expected to vary on a per residue basis as a function of  $\beta$ ,  $\gamma$ , and  $\theta$  (Equations 8–10), the extent of the effect will depend on the details of protein structure, e.g. on the distribution of peptide plane and NH bond orientations in the diffusion frame for a particular protein (Figure 5). For example, relative variations in  $R_1$  and  $R_2$  of the order of  $-5\%$  and  $+5\%$ , respectively, are expected to result in a 10% overestimation in the local  $R_2/R_1$  value. This in turn could lead to an  $\sim 5\%$  overestimation of the apparent overall correlation time, if all peptide planes were characterized by similar sets of the  $\{\beta, \gamma, \theta\}$  values, as one might anticipate, e.g., in helical bundles. In those cases when the  $\{\beta, \gamma, \theta\}$ -space is more uniformly sampled, both positive and negative sign variations in  $R_2/R_1$  are likely and the net effect on  $\tau_c$  might be reduced. However, site-specific variations in  $\gamma$  and  $\theta$  are expected to result in deviations in the apparent  $R_2/R_1$  vs.  $\beta$  dependence from the one expected under the assumption of collinear NH and CSA vectors. This is expected to affect both the preci-

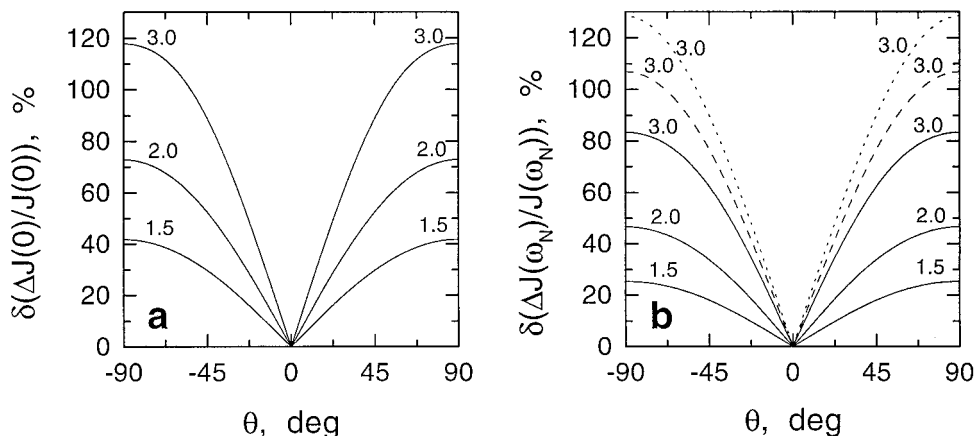


Figure 3. The maximal range of relative variations in (a)  $J(0)$  and (b)  $J(\omega_N)$  due to noncollinearity of the  $^{15}\text{N}$  CSA and  $^{15}\text{N}$ - $^1\text{H}$  dipolar interaction as a function of  $\theta$ , for various degrees of anisotropy,  $D_{\parallel}/D_{\perp}$ , indicated by numbers. The graphs represent  $\delta(\Delta J/J) = \max(\Delta J/J) - \min(\Delta J/J)$  for  $\beta, \gamma$  in the range from 0 to  $180^\circ$  (Figure 2). The data indicated by solid lines were obtained for a resonance frequency of 600 MHz, assuming the overall correlation time  $\tau_c$  of 5 ns. To illustrate the dependence of the effect on the field strength and on the overall correlation time, the dashed and dotted lines in (b) correspond to  $\tau_c = 10$  ns (at 600 MHz) and to 800 MHz ( $\tau_c = 5$  ns), respectively.

sion and accuracy of those methods of characterization of the overall rotational diffusion which are based on orientational dependence of  $R_2/R_1$  (Lee et al., 1997; Clore et al., 1998; Clore and Gronenborn, 1998). A model-independent analysis of  $^{15}\text{N}$  CSA was suggested recently (Fushman and Cowburn, 1998), based on the  $\eta/R_2$  ratio. Using this approach, we demonstrated (Fushman et al., 1998b) that the magnitude and orientation of the  $^{15}\text{N}$  CSA tensor in proteins can be determined from relaxation data in solution. The effect of anisotropy combined with noncollinearity of dipolar and CSA tensors was not considered. The effect on the ratio can be represented with the same approximations used above as:

$$\frac{\eta}{R_2} = \frac{2dcP_2(\cos\theta)}{d^2+c^2} \left\{ 1 + \frac{4\Delta J_{\text{CROSS}}(0, D_{\parallel}, D_{\perp}, \beta, \gamma, \theta) + 3\Delta J_{\text{CROSS}}(\omega_N, D_{\parallel}, D_{\perp}, \beta, \gamma, \theta)}{[4J_{DD}(0) + 3J_{DD}(\omega_N)]P_2(\cos\theta)} - \frac{c^2}{d^2+c^2} \frac{4\Delta J(0, D_{\parallel}, D_{\perp}, \beta, \gamma, \theta) + 3\Delta J(\omega_N, D_{\parallel}, D_{\perp}, \beta, \gamma, \theta)}{4J_{DD}(0) + 3J_{DD}(\omega_N)} \right\} \quad (15)$$

The terms containing  $\Delta J$  and  $\Delta J_{\text{CROSS}}$  describe additional effects of noncollinearity, and partially compensate each other. The residual contribution from these terms is proportional to the degree of rotational anisotropy and, for large  $\tau_c$  ( $\tau_c \gg 1/\omega_N$ ), does not depend on the molecular weight. Assuming CSA =  $-160$  ppm,  $\theta = -17^\circ$ , and  $\{\beta, \gamma\}$  in the  $0$ – $180^\circ$  range, the expected maximal variations in  $\eta/R_2$  at 600 MHz are 2%, 3.6%, and 6.4% for  $D_{\parallel}/D_{\perp} = 1.5, 2,$  and  $3$ , respectively. It can be shown that the primary effect

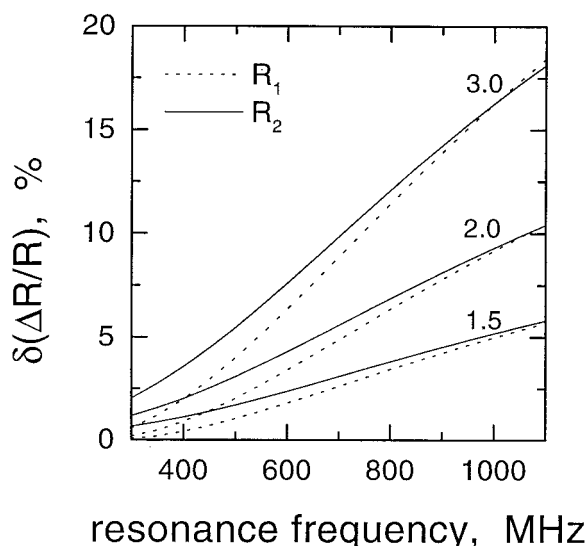


Figure 4. The maximal range of relative contributions to  $R_2$  (solid lines) and  $R_1$  (dotted lines) due to noncollinearity of the  $^{15}\text{N}$ - $^1\text{H}$  dipolar and  $^{15}\text{N}$  CSA tensors, as a function of resonance frequency, for various degrees of overall rotational anisotropy,  $D_{\parallel}/D_{\perp}$  (indicated in the figure). Shown is the difference between the greatest and the least values of  $[R(\Delta J) - R(0)]/R(0)$ , in percent, due to presence of the  $\Delta J$  terms in Equations 8 and 9, assuming CSA =  $-160$  ppm,  $\theta = -17^\circ$ , and  $\tau_c = 5$  ns.

of these variations in  $\eta/R_2$  is on the derived  $\theta$  values and not CSA. The expected changes in  $^{15}\text{N}$  CSA and  $\theta$  values for human ubiquitin derived using this extended  $\eta/R_2$  approach from those of (Fushman et al., 1998b) are very small, due to small rotational anisotropy;

maximum changes expected for  $\eta/R_2$  are  $\leq 1\%$ , of the order or less than the experimental errors. When the molecular parameters for  $\Delta J$ 's are available, exact derivation of CSA values using Equation 15 for the cases of significant rotational anisotropy is practical.

Similar considerations can be applied to assess the effect of noncollinearity of the  $^{13}\text{C}$  CSA and  $^{13}\text{C}'\text{-}^{13}\text{C}\alpha$  dipolar tensor on carbonyl relaxation in uniformly  $^{13}\text{C}$ -labeled proteins (Fischer et al., 1997).

The noncollinearity of the  $^{15}\text{N}$  CSA and  $^1\text{H}\text{-}^{15}\text{N}$  dipolar tensors is also expected to have a significant effect on relaxation-optimized experimental approaches, such as TROSY (Pervushin et al., 1997, 1998). The TROSY resonance line width (at half height) in the  $^{15}\text{N}$  dimension for amide groups is  $\Delta\nu(^{15}\text{N}) = \pi^{-1}(R_2 - \eta)$  Hz, where only contributions to relaxation from interactions within the amide group are considered. Using Equations 9 and 13 and neglecting the high-frequency components of  $J(\omega)$  in Equation 9, it can be recast as follows:

$$\begin{aligned} \Delta\nu(^{15}\text{N}) = & \pi^{-1}\left\{\frac{1}{2}[d^2 + c^2 \right. \\ & - 2dcP_2(\cos\theta)][4J_{DD}(0) + 3J_{DD}(\omega_N)] \\ & + \frac{1}{2}c^2[4\Delta J(0, D_{||}, D_{\perp}, \beta, \gamma, \theta) \\ & + 3\Delta J(\omega_N, D_{||}, D_{\perp}, \beta, \gamma, \theta)] \\ & - dc[4\Delta J_{\text{CROSS}}(0, D_{||}, D_{\perp}, \beta, \gamma, \theta) \\ & \left. + 3\Delta J_{\text{CROSS}}(\omega_N, D_{||}, D_{\perp}, \beta, \gamma, \theta)]\right\} \quad (16) \end{aligned}$$

How does this affect the TROSY experiment? For spherical proteins, all  $\Delta J$ 's vanish, and the optimal conditions for TROSY are:  $c = dP_2(\cos\theta)$ , which gives  $B_o(\text{opt}) = -(\mu_o/(4\pi))3\gamma_{\text{H}}hP_2(\cos\theta)[4\pi r_{\text{HN}}^3(\sigma_{||} - \sigma_{\perp})]^{-1}$ . A nonzero angle  $\theta$  (hence  $P_2(\cos\theta) < 1$ ) will shift the optimal resonance frequency towards lower values than expected for collinear  $^{15}\text{N}$  CSA and  $^1\text{H}\text{-}^{15}\text{N}$  dipolar tensors. Assuming CSA =  $-160$  ppm,  $r_{\text{HN}} = 1.02$  Å, and  $\theta = -17^\circ$ , the optimal resonance frequency is 924 MHz, compared to 1.06 GHz for  $\theta = 0$ . The residual TROSY linewidth at the optimal conditions (further referred to as  $\Delta\nu_o$ ) is expected to be proportional to protein molecular weight, and is predicted to be 1.6, 4.7, and 25 Hz, for spherical proteins with molecular weights of 50, 150, and 800 kDa ( $\tau_c$  of 20, 60, and 230 ns (Wüthrich, 1998)). When rotational anisotropy is present, the  $\Delta J$ -terms also contribute to the observed  $\Delta\nu(^{15}\text{N})$ , their contribution being proportional to  $(D_{||}/D_{\perp} - 1)$  and to molecular weight. All terms in

Equation 16 are orientationally dependent. The resulting linewidth is expected to vary for different amide groups' geometries, reflecting structure-specific variations in the NH-bond and CSA tensor orientations ( $\beta$ ,  $\gamma$  angles) with respect to the rotational diffusion axes. The calculated  $\Delta\nu(^{15}\text{N})$  range, in per cent of  $\Delta\nu_o$ , is from 88 to 112%, 81–126%, 73–153%, and 67–208% for  $D_{||}/D_{\perp} = 1.5, 2, 3$ , and 5, respectively. In addition, site-specific variations in the local orientation ( $\theta$  angle) as well as in the magnitude of the  $^{15}\text{N}$  CSA tensor (Fushman et al., 1998b) will also alter the observed linewidths. For example, for isotropic rotational diffusion,  $\pm 5^\circ$  variations in  $\theta$  will result in the actual linewidths ranging from 54% to 160% of  $\Delta\nu_o$  (e.g. 2.6 to 7.6 Hz for  $\tau_c = 60$  ns); whereas  $\pm 40$  ppm variations in CSA magnitude are expected to cause only up to a 20% increase in  $\Delta\nu_o$ ; similar numbers characterize an increase in the  $\Delta\nu(^{15}\text{N})$  range in the case of rotational anisotropy.

These calculations suggest that the effect of noncollinearity of the  $^{15}\text{N}$  CSA and  $^1\text{H}\text{-}^{15}\text{N}$  dipolar interactions on the TROSY linewidth might become significant for proteins with high degree of rotational anisotropy and large molecular weight. This will affect the ability to observe all amides with equal efficiency in the TROSY experiment. On the other hand, this might provide a valuable source of structural information (on  $\theta$ ,  $\beta$ ,  $\gamma$ ) encoded in the linewidths/intensities according to Equation 16.

More complex models of molecular shape and motion than the ellipsoid model used here are obviously possible, and the approach of Equations 3–13 could be generalized.

## Conclusions

Current approaches to  $^{15}\text{N}$  relaxation in proteins assume that the  $^{15}\text{N}\text{-}^1\text{H}$  dipolar and  $^{15}\text{N}$  CSA tensors are collinear. It is shown here that different orientation of the two tensors, experimentally observed in proteins, nucleic acids, and small peptides will result in differences in NMR-relevant autocorrelation functions and spectral densities characterizing reorientation of the  $^{15}\text{N}\text{-}^1\text{H}$  dipolar and of the  $^{15}\text{N}$  CSA tensors in the case of anisotropic overall rotation. The standard treatment of the rates of longitudinal and transverse relaxation of amide  $^{15}\text{N}$  nuclei is extended in order to account for the effect of noncollinearity of the  $^{15}\text{N}\text{-}^1\text{H}$  dipolar and  $^{15}\text{N}$  CSA tensors. This effect shown to be proportional to the degree of anisotropy of the overall motion,

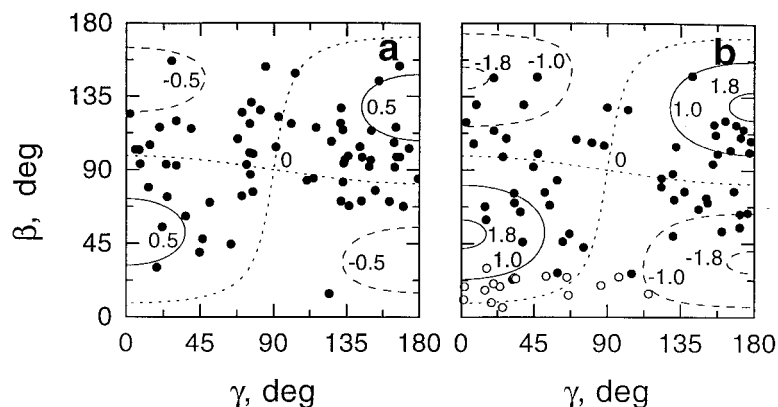


**Figure 5.** Two examples of a distribution of  $\{\beta, \gamma\}$  values in proteins: (a) human ubiquitin and (b) Pleckstrin Homology (PH) domain of  $\beta$ -adrenergic receptor kinase ( $\beta$ ARK, PDB entry 1bak) (Fushman et al., 1998a). Symbols indicate the location of each individual amide group on the  $\{\beta, \gamma\}$  map. Lines represent contour levels (indicated with numbers (%)) for 600 MHz of the relative deviation,  $[R_2(\Delta J)/R_1(\Delta J) - R_2(0)/R_1(0)]/[R_2(0)/R_1(0)]$ , of the  $R_2/R_1$  ratio due to the effect of noncollinearity. In (b), residues 87–104 belonging to the  $\alpha$ -helix of  $\beta$ ARK are indicated with open circles, while the rest of the protein is shown as solid circles, to illustrate the nonuniform distribution of NH bonds orientation because the unique axis of the diffusion tensor is nearly parallel to the helical axis (Fushman et al., 1998a). Atom coordinates for ubiquitin are from the crystal structure (PDB entry 1ubq); hydrogen atoms were added using Insight II (Biosym). For both ubiquitin and  $\beta$ ARK structures, the deviations of the  $\text{NH}_i$  bond from the  $C'_{i-1}\text{-N}_i\text{-C}_{\alpha i}$  plane were less than  $0.3^\circ$ . The rotational anisotropy of the proteins, determined from  $^{15}\text{N}$  relaxation studies, is characterized by  $D_{\parallel}/D_{\perp} = 1.17$  for ubiquitin (Tjandra et al., 1995) and 1.35 for  $\beta$ ARK PH domain (Fushman et al., 1998a). Residues located in highly flexible termini (residues 73–76 in ubiquitin, 1–9 and 106–119 in  $\beta$ ARK) and flexible loops (18–26, 42–48, and 74–76 in  $\beta$ ARK) are not shown. While the effect of noncollinearity is below the level of experimental uncertainty in the  $^{15}\text{N}$  relaxation data reported for ubiquitin (Tjandra et al., 1995), it increases linearly with  $(D_{\parallel}/D_{\perp} - 1)$  and is comparable to the experimental uncertainty for the  $\beta$ ARK PH domain.

$D_{\parallel}/D_{\perp} - 1$ , is sensitive to orientation of the peptide plane with respect to the diffusion tensor frame. Although negligible at small degrees of anisotropy, the effect is predicted to become significant for  $D_{\parallel}/D_{\perp} \geq 1.5$  and at high magnetic fields.

The effect of noncollinearity of  $^{15}\text{N}$  CSA and  $^{15}\text{N}$ - $^1\text{H}$  dipolar interaction is therefore expected to be sensitive to both gross (hydrodynamic) properties and atomic-level details of protein structure. Incorporation of this effect into relaxation data analysis is likely to improve both precision and accuracy of the derived characteristics of protein dynamics, especially at high magnetic fields and for molecules with high degree of anisotropy of the overall motion. The effect might prove useful for relaxation-optimized experimental approaches which rely on matching dipolar and CSA contributions, like TROSY (Pervushin et al., 1997).

### Acknowledgements

We are grateful to Prof. A.G. Palmer III for stimulating discussion. The authors acknowledge the support of grant NIH GM-47021.

### Notes added during revision

After this paper was submitted, a paper became available on the J. Am. Chem. Soc. web page (Boyd and Redfield, 1998), where the authors present a similar idea of differences between the spectral density functions describing contributions to amide  $^{15}\text{N}$  relaxation from reorientations of  $^1\text{H}$ - $^{15}\text{N}$  dipolar interaction and  $^{15}\text{N}$  CSA. They show that an introduction of the angle between the CSA and dipolar vectors as an additional fitting parameter, assumed to be uniform throughout the protein, in combination with the axially symmetric rotational diffusion model, leads to an improved agreement between the experimental and calculated  $T_2/T_1$  ratios for hen lysozyme.

### References

- Abragam, A. (1961) *The Principles of Nuclear Magnetism*, Clarendon Press, Oxford.
- Akke, M., Brüschweiler, R. and Palmer, A. (1993) *J. Am. Chem. Soc.*, **115**, 9832–9833.
- Boyd, J. and Redfield, C. (1998) *J. Am. Chem. Soc.*, **120**, 9692–9693.
- Bremi, T., Brüschweiler, R. and Ernst, R.R. (1997) *J. Am. Chem. Soc.*, **119**, 4272–4284.



- Brink, D.M. and Satchler, G.R. (1993) *Angular Momentum*, Clarendon Press, Oxford.
- Chatfield, D.C., Szabo, A. and Brooks, B.R. (1998) *J. Am. Chem. Soc.*, **120**, 5301–5311.
- Clore, G.M. and Gronenborn, A.M. (1998) *Proc. Natl. Acad. Sci. USA*, **95**, 5891–5898.
- Clore, G.M., Gronenborn, A.M., Szabo, A. and Tjandra, N. (1998) *J. Am. Chem. Soc.*, **120**, 4889–4890.
- Fischer, M.W.F., Zeng, L., Pang, Y., Hu, W., Majumdar, A. and Zuiderweg, E.R.P. (1997) *J. Am. Chem. Soc.*, **119**, 12629–12642.
- Fushman, D., Ohlenschläger, O. and Rüterjans, H. (1994) *J. Biomol. Struct. Dyn.*, **4**, 61–78.
- Fushman, D. and Cowburn, D. (1998) *J. Am. Chem. Soc.*, **120**, 7109–7110.
- Fushman, D., Najmabadi-Haske, T., Cahill, S.M., Zheng, J., LeVine, H.A., III and Cowburn, D. (1998a) *J. Biol. Chem.*, **273**, 2835–2843.
- Fushman, D., Tjandra, N. and Cowburn, D. (1998b) *J. Am. Chem. Soc.*, **120**, 10947–10952.
- Goldman, M. (1984) *J. Magn. Reson.*, **60**, 437–452.
- Harbison, G.S., Jelinski, L.W., Stark, R.E., Torchia, D.A., Herzfeld, J. and Griffin, R.G. (1984) *J. Magn. Reson.*, **60**, 79–82.
- Hartzell, C.J., Whitfield, M., Oas, T.G. and Drobny, G.P. (1987) *J. Am. Chem. Soc.*, **109**, 5966–5969.
- Hiyama, Y., Niu, C., Silverton, J., Bavoso, A. and Torchia, D. (1988) *J. Am. Chem. Soc.*, **110**, 2378–2383.
- Kay, L.E., Nicholson, L.K., Delaglio, F., Bax, A. and Torchia, D. (1992) *J. Magn. Reson.*, **97**, 359–375.
- Kay, L.E., Torchia, D.A. and Bax, A. (1989) *Biochemistry*, **28**, 8972–8979.
- Lee, L.K., Rance, M., Chazin, W.J. and Palmer, A.G., III (1997) *J. Biomol. NMR*, **9**, 287–298.
- Mai, W., Hu, W., Wang, C. and Cross, T.A. (1993) *Protein Sci.*, **2**, 532–542.
- Oas, T.G., Hartzell, C.J., Dahlquist, F.W. and Drobny, G.P. (1987) *J. Am. Chem. Soc.*, **109**, 5962–5966.
- Ottiger, M., Tjandra, N. and Bax, A. (1997) *J. Am. Chem. Soc.*, **119**, 9825–9830.
- Palmer, A., Sketon, N., Chazin, W., Wright, P. and Rance, M. (1992) *Mol. Phys.*, **75**, 699–711.
- Peng, J. and Wagner, G. (1992) *J. Magn. Reson.*, **94**, 82–100.
- Pervushin, K., Riek, R., Wider, G. and Wüthrich, K. (1997) *Proc. Natl. Acad. Sci. USA*, **94**, 12366–12371.
- Pervushin, K., Riek, R., Wider, G. and Wüthrich, K. (1998) *J. Am. Chem. Soc.*, **120**, 6394–6400.
- Shoji, A., Ozaki, T., Fujito, T., Deguchi, K., Ando, S. and Ando, I. (1989) *Macromolecules*, **22**, 2860–2863.
- Tjandra, N., Feller, S.E., Pastor, R.W. and Bax, A. (1995) *J. Am. Chem. Soc.*, **117**, 12562–12566.
- Tjandra, N., Garrett, D.S., Gronenborn, A.M., Bax, A. and Clore, G.M. (1997) *Nat. Struct. Biol.*, **4**, 443–449.
- Tjandra, N., Szabo, A. and Bax, A. (1996) *J. Am. Chem. Soc.*, **118**, 6986–6991.
- Woessner, D. (1962) *J. Chem. Phys.*, **37**, 647–654.
- Wüthrich, K. (1998) *Nat. Struct. Biol.*, **5** Suppl, 492–495.
- Yang, D. and Kay, L.E. (1996) *J. Mol. Biol.*, **263**, 369–382.